Cell Death and Differentiation (1998) 5, 432–439

http://www.stockton-press.co.uk/cdd

Comparative effects of Bcl-2 over-expression and ZVAD.FMK treatment on dexamethasone and VP16-induced apoptosis in CEM cells

Roderick Simon Patrick Benson[1], Caroline Dive[1] and Alastair John Mackenzie Watson[2]

[1] School of Biological Sciences, The University of Manchester, Oxford Road, Manchester, UK
[2] Department of Medicine, The University of Manchester, Oxford Road, Manchester, UK
[3] corresponding author: A.J.M. Watson, G38, Stopford Building, The University of Manchester, Oxford Road, Manchester, M20 9PT, Tel: +(0)161 787 4560; Fax +(0)161 275 5600; email: alastair.watson@man.ac.uk

Received 17.7.97; revised 13.11.97; accepted 5.12.1997
Edited by M. Piacentina

Abstract

It is becoming apparent that caspases are essential mediators of the execution phase of apoptosis. A decrease in mitochondrial membrane potential (Ψ_M) is also thought to be an early event in apoptosis. In this study, we compare the effects of Bcl-2 over-expression against N-benzyloxycabonyl-Val-Ala-Asp-fluoromethylketone (ZVAD.FMK)-sensitive caspase blockade on dexamethasone (DEX) and etoposide (VP16)-induced apoptosis in CEM T lymphoid cells. We assessed changes in nuclear chromatin, cell size, fragmentation, cell membrane permeability and Ψ_M. We found Bcl-2 over-expression and ZVAD.FMK-sensitive caspase inhibition were able to prevent chromatin condensation and cellular fragmentation. However, ZVAD.FMK was neither able to prevent loss of plasma membrane integrity nor Ψ_M depolarization which occur in both VP16 and DEX-induced apoptosis. In VP16-induced apoptosis, the increase in cell membrane permeability was actually potentiated by caspase inhibition. Interestingly, ZVAD.FMK did prevent VP16-induced but not DEX-induced cell shrinkage. These results suggest that not all the actions of Bcl-2 can be explained by its ability to prevent caspase activation. Rather Bcl-2 must have other targets of action which include functions associated with mitochondria.

Keywords: apoptosis; cell death; necrosis; caspases; Bcl-2; caspase inhibitors

Abbreviations: dexamethasone, DEX; etoposide, VP16; N-benzyloxycabonyl-Val-Ala-Asp-fluoromethylketone, ZVAD.FMK; N-benzyloxycabonyl-Asp-Glu-Val-L-Asp-fluoromethylketone, DEVD.FMK; mitochondrial membrane potential, Ψ_M; apoptosis initiating factor, AIF; permeability transition, PT; weighted median volume, WMV

Introduction

Apoptosis is a structurally defined programmed cell death which plays an essential role in development and tissue homeostasis (Arends and Wyllie, 1991). Recent work has shown that Bcl-2 family members, mitochondria and caspases play key roles in the regulation and execution of apoptosis. Over-expression of Bcl-2 or inhibition of caspases can suppress or at least delay the onset of apoptosis in several cell types (Oltvai and Korsmeyer, 1994; Meisenholder *et al*, 1996; Decaudin *et al*, 1997). Thus, we set out to determine whether the effects of Bcl-2 could be completely recapitulated by inhibition of caspases in a well characterised T cell model system. Exposure to agents which induce apoptosis activate signal transduction pathways which culminate in the release of cytochrome C, Apoptosis Initiating Factor (AIF) and possibly other compounds from the mitochondria (Zamzami *et al*, 1996; Golstein, 1997; Kluck *et al*, 1997). In most systems, these mitochondrial derived substances are believed to somehow activate caspases which cleave specific substrates causing the structural changes of apoptosis. It is not understood how these substances are released but it may involve the induction of the mitochondrial megapore or permeability transition (Zamzami *et al*, 1995). This can be detected experimentally in whole cells as a loss of mitochondrial potential. Bcl-2, and some of the other family members, are tethered to the outer mitochondrial membrane and can prevent the induction of permeability transition and the release of cytochrome C and AIF (Zamzami *et al*, 1996; Yang *et al*, 1997). It is argued that this action of Bcl-2 will prevent the subsequent activation of the caspases thereby blocking apoptotic cell death (Kroemer, 1997).

In order to test this hypothesis, we examined cell shrinkage and fragmentation, plasma membrane integrity and Ψ_M in the presence of the general caspase inhibitor ZVAD.FMK to establish whether the effects of Bcl-2 on these parameters were mimicked by the inhibition of ZVAD.FMK-sensitive caspases. Given, a recent study which suggests that the ordering of the regulation events may depend on the initiation stimulus (Boise and Thompson, 1997), we also examined the same parameters in etoposide-induced apoptosis to determine whether the changes following exposure to DEX, and their modulation by two distinct apoptotic inhibitors (Bcl-2 and ZVAD.FMK), are general feature of apoptosis. We found that the actions of Bcl-2 were not fully recapitulated by the inhibition of ZVAD.FMK-sensitive caspases. In particular, although over-expression of Bcl-2 and ZVAD.FMK-sensitive caspases both block chromatin condensation and cellular fragmentation, only over-expression of Bcl-2 blocked the loss in Ψ_M implying that mitochondrial changes are upstream of caspase action in

this cellular setting. Furthermore, Bcl-2 over-expression, but not blockade of ZVAD.FMK-sensitive caspases, prevented loss of membrane permeability. This later result implies that Bcl-2 must have other functions within the cell other than the prevention of caspase activation in the suppression of apoptosis.

Results

The effect of caspase inhibition or Bcl-2 over-expression on cell volume and chromatin condensation

As with CEM-C7A cells which we have studied previously (Benson *et al*, 1996), CEM_{neo} cells displayed a slow time course for the onset of apoptosis, with nuclear changes apparent after 48 h of continuous treatment with DEX (5 μM). The number of cells with condensed chromatin then increased steadily to a maximum of 76$\pm$8% (mean$\pm$S.E.M.) at 96 h. Enforced over-expression of Bcl-2 inhibited chromatin condensation completely (Figure 1A). In contrast to the nuclear changes, Bcl-2 over-expression did not prevent cell shrinkage observed during the first 24 h of exposure to DEX (Figure 1A) although, at later time points, the rate at which the weighted median volume (WMV) decreases for $CEM_{Bcl\text{-}2}$ was less than in the CEM_{neo} cell populations. For example, after exposure to DEX for 48 h, the WMV of CEM_{neo} cells was significantly less than the WMV of $CEM_{Bcl\text{-}2}$ cells (WMV of CEM_{neo}=497$\pm$11.6 fl and $CEM_{Bcl\text{-}2}$=562.9$\pm$11.7 fl, n=5, P=0.0039) and this difference was maintained over the subsequent time course of the experiment. In contrast to the action of Bcl-2, inhibition of caspases with ZVAD.FMK (50 μM) added 24 h after addition of DEX did not prevent either phase 1 or phase 2 cell shrinkage although the appearance of cells with chromatin condensation was blocked (Figure 1B). Similar results were obtained when DEX and ZVAD.FMK were added simultaneously. This demonstrates that in DEX-induced apoptosis the anti-apoptotic effects of Bcl-2 are not entirely mediated through ZVAD.FMK-sensitive caspases.

We have shown previously that cell shrinkage occurs in two phases in DEX-induced apoptosis. The first phase of cell volume loss occurs synchronously to all cells in the population before chromatin condensation takes place. The second phase occurs concurrently with chromatin condensation and is partly accounted for by cellular fragmentation; (cell volume changes are illustrated in panels 1 and 2 of Figure 1C). Population 'a' in panel 2 corresponds to cells with normal morphology which have shrunk synchronously compared to untreated cells in panel 1. Neither over-expression of Bcl-2 (panel 3) nor exposure to 50 μM ZVAD.FMK (panel 4) prevented this first phase of volume loss. For example, the cell size of subpopulation 'a' in the DEX-treated CEM_{neo} cells (panel 2) is similar to the median cell size for the whole $CEM_{Bcl\text{-}2}$ cell population (panel 3). Cell population 'b' (panel 2) corresponds to cells with apoptotic nuclear morphology and population 'c' represents cell fragments (previously proved by cell sorting Benson *et al*, 1996). Appearance of these subpopulations was largely prevented by over-expression of Bcl-2. Thus while $CEM_{Bcl\text{-}2}$ cells undergo a DEX-induced phase 1 volume loss, the second phase of volume loss associated with the onset of chromatin condensation is prevented. This explains the partial block of WMV loss by over-expression of Bcl-2 as

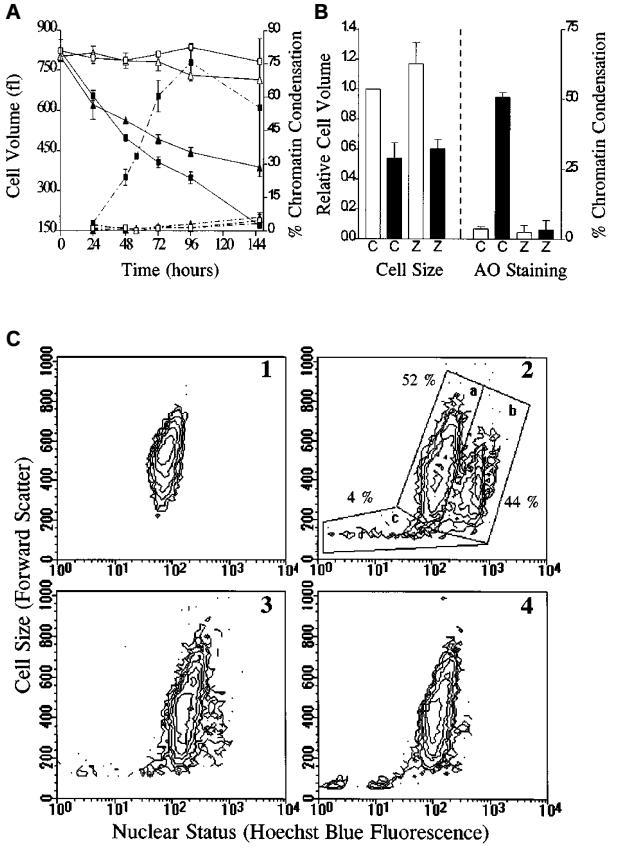

Figure 1 (**A**) Time course for cell shrinkage (*normal lines*) and chromatin condensation (*dotted lines*) in CEM_{neo} (*squares*) and $CEM_{Bcl\text{-}2}$ cells (*triangles*) treated for up to 147 h with 5 μM DEX (*closed symbols*) or 0.1% v/v ethanol as a vehicle control (*open symbols*). Cell volume was measured using Coulter counter electronic cell sizing and is expressed in fl (10^{-15} l, left ordinate) and chromatin condensation was assessed using the nuclear dye acridine orange and is expressed as the percentage of cells which appeared to have a condensed nucleus under the microscope (right ordinate, see methods). Each data point represents the mean$\pm$S.E.M. of at least four experiments. (**B**) Bar graph showing the effect of ZVAD.FMK on cell DEX-induced cell shrinkage and chromatin condensation at 72 h. The white and black bars represent the mean$\pm$S.E.M. of three experiments for ethanol, acting as a vehicle control (*white bars*), or 5 μM DEX (*black bars*). Bars labelled 'Z' are cell cultures that were treated with 50 μM ZVAD.FMK which was added 24 h after the initial exposure to DEX. Bars labelled 'C' represent the parallel controls which received DMSO vehicle only (0.1% v/v). Cell volume was measured by flow cytometry as described previously (Benson *et al*, 1996) and each condition normalised to the ethanol-DMSO vehicle control (relative volume for this is 1.0 by definition). Chromatin condensation was ascertained by AO staining as described in Figure 1A. (**C**) Multiparameter flow cytometric analysis of cell shrinkage and chromatin condensation in CEM_{neo} cells (*panels 1, 2 and 4*) and $CEM_{Bcl\text{-}2}$ cells (*panel 3*) treated with 5 μM DEX for 72 h. CEM_{neo} cells treated with DEX only undergo substantial apoptosis after 72 h (*panel 2*). Loading Ho342 for only a short time results in apoptotic cells staining more intensely with the nuclear dye and so they appear in the second gate marked [b] in panel 2. Cells in population [a] have normal nuclei while events in population [c] have reduced forward scatter signal and thus represents cell fragments. Appearance of subpopulations [b] and [c] are nearly completely blocked by Bcl-2 over-expression (*panel 3*) or by incubating the cells with ZVAD.FMK (50 μM) for 48 h after the initial 24 h of DEX exposure (*panel 4*). The ZVAD.FMK vehicle control was DMSO (0.1% v/v). These data are representative of at least three individual experiments

noted in Figure 1A. In contrast, although exposure to 50 μM ZVAD.FMK (panel 4) prevented appearance of population 'b' there was further loss of volume in the single population so, overall, ZVAD.FMK had no effect on the population median cell volume (Figure 1B).

To further confirm that there was a phase of cell shrinkage which was Bcl-2 sensitive we induced apoptosis in CEM cells using the DNA damaging agent VP16. Unlike the observation seen with DEX, VP16 initially induced a slight cell swelling followed by cell shrinkage which occurred concurrently with chromatin condensation with this apoptotic stimulus. Both Bcl-2 over-expression and 50 μM ZVAD.FMK completely inhibited cell shrinkage and chromatin condensation (Figure 2A,B). Multiparameter flow analysis confirmed these results. Bcl-2 over-expression prevented the appearance of the apoptotic cell subpopulation (marked 'b' in Figure 2C, panel 2) and ZVAD.FMK caused a substantial decrease in the number of cells within population 'b' (Figure 2C, panel 4). Thus, during VP16-induced apoptosis there appeared to be a single mechanism of cell volume loss which is inhibited by Bcl-2 over-expression and ZVAD.FMK-sensitive caspase inhibition.

The caspase inhibitor ZVAD.FMK not only inhibits ICE like proteases but it also can indirectly inhibit CPP32 by blocking its activation in living cells (Slee *et al*, 1996). In contrast, the fluoromethylketone derivative of Asp-Glu-Val-L-Asp (DEVD.FMK) is more specific for CPP32 (caspase-3) which is believed to be one of the main mediators of apoptosis (Cohen, 1997). We examined whether a more specific blockade of caspase-3 would be similar to the general inhibition of caspases by ZVAD.FMK. Surprisingly, we were unable to achieve a satisfactory inhibition of either DEX or VP16-induced caspase-3 activity even when the inhibitor was used at a dose of 150 μM (Figure 3). In contrast, ZVAD.FMK at a dose of 50 μM was able to completely inhibit PARP cleavage induced by either VP16 (Figure 3A) or DEX (Figure 3B). Since ZVAD.FMK was the most effective agent at inhibiting caspase-mediated PARP cleavage the remainder of our studies were performed using this inhibitor as a comparison for the anti-apoptotic effects of Bcl-2 over-expression.

One limitation with population measurements of cell volume is that they do not give any information on the precise time it takes for an individual cell to reduce its cellular volume. We addressed this issue using video microscopy of VP16-induced apoptosis. As previously described (McCarthy

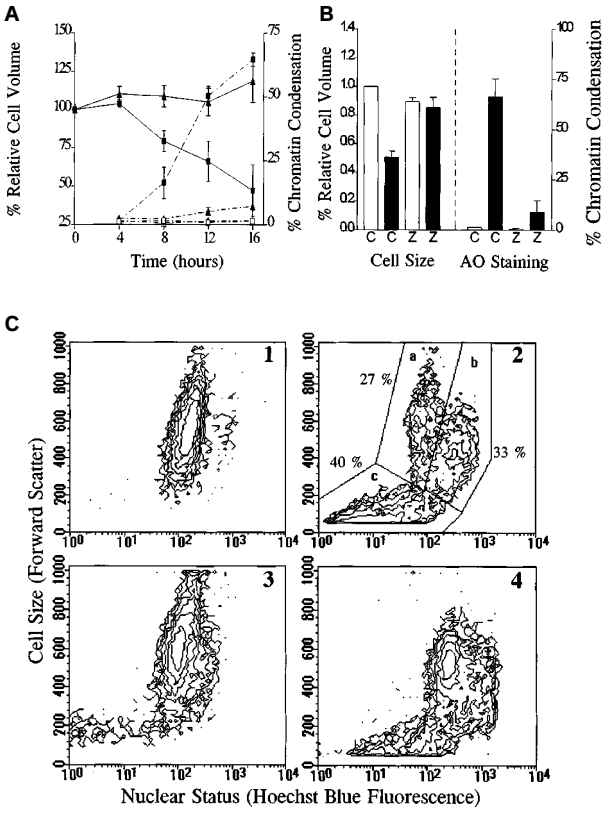

Figure 2 (**A**) Time course for cell shrinkage (*normal lines*) and chromatin condensation (*dotted lines*) in CEM_{neo} (*squares*) and CEM_{Bcl-2} cells (*triangles*) treated for up to 16 h with 5 μM VP16 (*closed symbols*) or an equivalent volume of DMSO, acting as a vehicle control (*open symbols*). Cell volume relative to controls was measured using flow cytometry as described in Figure 1B so only the treated relative cell volumes (*closed symbols*) are shown as control cell volumes are 100% by definition. AO staining is the same for Figure 1A. Each data point represents the mean $\pm$ S.E.M. of at least four experiments. (**B**) Bar graph showing the effect of ZVAD.FMK on cell VP16-induced cell shrinkage and chromatin condensation after 16 h. The white and black bars represent the mean $\pm$ S.E.M of three experiments for vehicle control (*white bars*), or 5 μM VP16 (*black bars*). Bars labelled 'Z' are cell cultures that were treated with 50 μM ZVAD.FMK and which was added at the beginning of the experiment. Bars labelled 'C' represent the parallel controls which received DMSO vehicle only. Cell size and chromatin condensation was measured as described in Figure 1B. (**C**) Multiparameter flow cytometric analysis of cell shrinkage and chromatin condensation in CEM_{neo} cells (*panels 1, 2 and 4*) and CEM_{Bcl-2} cells (*panel 3*) treated with 5 μM VP16 for 16 h. CEM_{neo} cells treated with VP16 only, undergo substantial apoptosis after 16 h (*panel 2*) and the cell subpopulations which result are labelled as described in Figure 1C. Subpopulations B and C are nearly completely blocked by Bcl-2 over-expression (*panel 3*) and substantially decreased by co-incubating the cells with ZVAD.FMK (50 μM) for 16 h (*panel 4*). These data are representative of at least three individual experiments

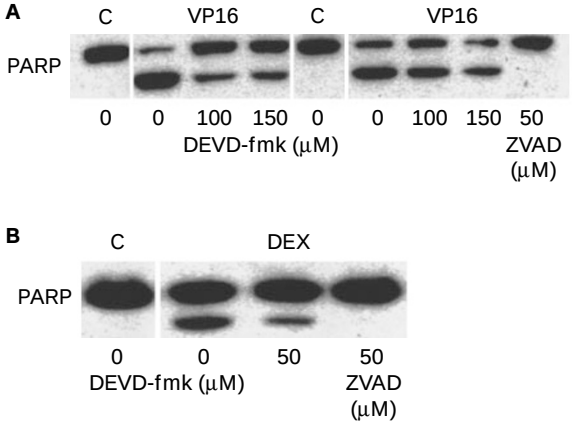

Figure 3 The effect of DEVD.FMK and ZVAD.FMK on PARP cleavage. Cell lysates were prepared from CEM_{neo} cells treated for 16 h with 5 μM VP16 (*panel A*) or 72 h with 5 μM DEX (*panel B*). Lanes marked with 'C' represent vehicle controls which received 0.1% v/v of ethanol or DMSO for DEX or VP16 respectively. The doses of DEVD.FMK are also indicated on the figure with the 0 μM doses receiving 0.4% DMSO as a vehicle control. The lanes furthest to the right in the two panels are blots from cell lysates treated with ZVAD.FMK (50 μM) as described in Figures 1B and 2B for DEX and VP16 respectively

et al, 1997) cell shrinkage was rapid and was associated with rapid shape changes and the appearance of blebs on the cell surface. The mean length of time from the onset of cell shrinkage to its completion was 12.4±0.9 min in CEM_{neo} (mean±S.E.M., 12 cells from 1 experiment).

The effect of Bcl-2 and ZVAD.FMK on cellular fragmentation and cell membrane integrity

Multiparameter flow-cytometric plots which show the effect of Bcl-2 and ZVAD.FMK on DEX-induced cellular fragmentation and cell membrane permeability are presented in Figure 4A. Figures 4B and C are the corresponding bar charts which summarize the data from three independent multiparameter flow-cytometric experiments. Exposure of CEM_{neo} cells to DEX (5 μM) for 72 h (Figure 4A, panel 2) caused both a loss of plasma membrane integrity resulting in red fluorescence due to the entry of propidium (Events coded as black) and cellular fragmentation (Coded as dark grey in population F). Bcl-2 completely inhibited DEX-induced cellular fragmentation and loss of cell membrane integrity (Figure 4A panel 3; Figure 4B) while ZVAD.FMK prevented fragmentation but not cell membrane integrity loss (Figure 4A panel 4; Figure 4C). Figure 5B and C show the equivalent data for CEM cells treated with VP16. Bcl-2 attenuated fragmentation significantly ($P<0.01$, $n=3$) after 16 h of drug exposure (Figure 5A panel 3; Figure 5B) but this effect was only temporary because fragmentation at 24 h was not significantly different between the neo and Bcl-2 cell lines (data not shown). Loss of cell membrane integrity, following exposure to 5 μM VP16, only developed at the later time points but was also attenuated by Bcl-2 over-expression (56±24% *vs* 20±5% for CEM_{neo} and $CEM_{Bcl\text{-}2}$ respectively, $P<0.01$ at 24 h, $n=3$). However, again this effect was only temporary, as examination of $CEM_{Bcl\text{-}2}$ cells after 48 h of VP16 exposure indicated

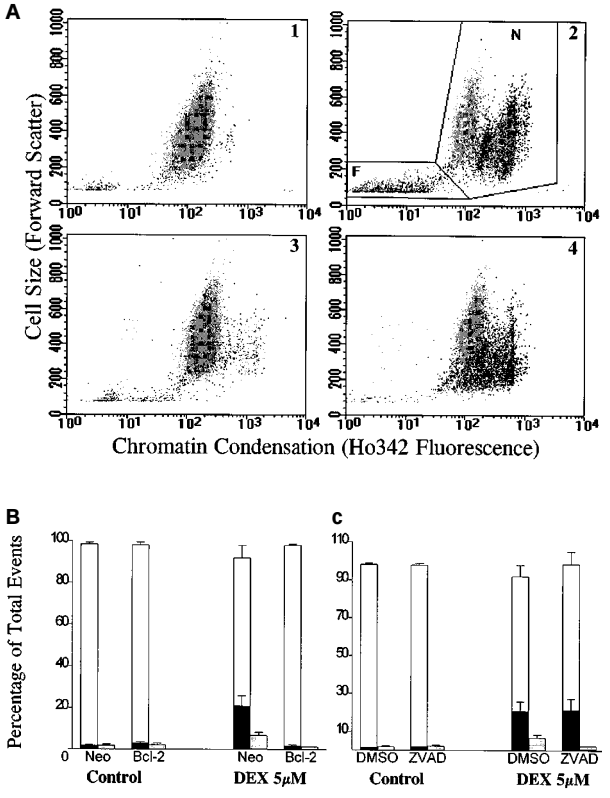

Figure 4 (**A**) Analysis of cellular fragmentation and loss of cell membrane integrity in CEM cells treated with 5 μM DEX, or an equivalent volume of ethanol, acting as a vehicle control for 72 h. Cells were incubated with the dyes Ho342 (10 μM) and PI (32 μM) for 5 min before analysing using flow cytometry. The data is presented as 2D-dot plots with cell size (forward scatter) on the ordinate and Ho342 fluorescence on the abscissa. Particle forward scatters below 200 channel units are designated fragments (labelled [F] in panel 2) and colour coded dark grey. Cells which allow the entry of PI are colour coded black and the remaining events (located in the gate labelled [N]) are coded light grey. The four experimental conditions shown are CEM_{neo} cells treated with vehicle controls (*panel 1*), CEM_{neo} cells treated with DEX (*panel 2*), $CEM_{Bcl\text{-}2}$ cells treated with DEX (*panel 3*) and CEM_{neo} cells treated with DEX and ZVAD.FMK as described in Figure 1B (*panel 4)* (**B** and **C**) Bar graphs showing the numerical summary of multiparameter flow-cytometry experiments presented in Figure 3A. The white bars represents all events in gate [N] the grey bar represents all events in gate [F] (i.e. fragments) and the black bars represents the percentage of events in either population which are positive to PI. Each bar represents the mean±S.E.M. of three experiments for apoptosis blocked by Bcl-2 over-expression (**B**) or caspase inhibition (**C**)

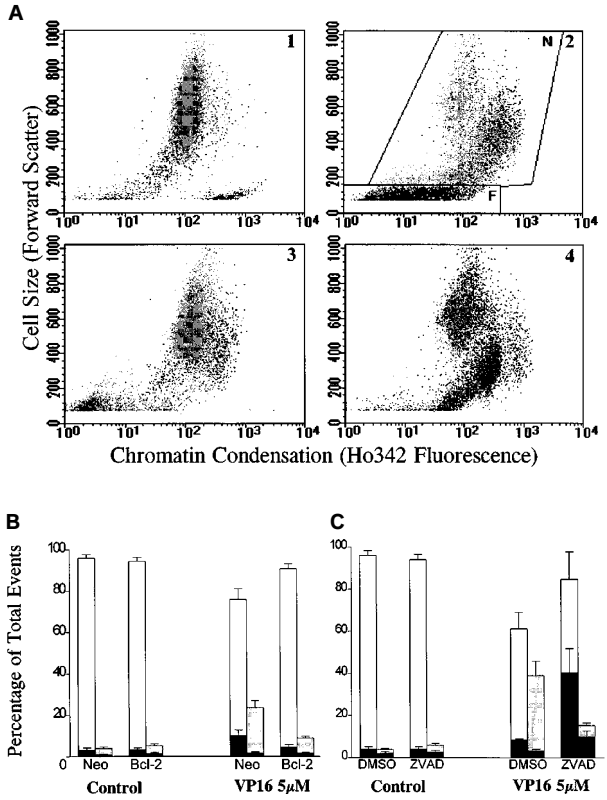

Figure 5 (**A**) Analysis of cellular fragmentation and loss of cell membrane integrity in CEM cells treated with 5 μM VP16, or an equivalent volume of DMSO, acting as a vehicle control for 16 h. The experimental conditions and gating is the same as that described in Figure 4. The four experimental conditions shown are CEM_{neo} cells treated with vehicle controls (*panel 1*), CEM_{neo} cells treated with VP16 (*panel 2*), $CEM_{Bcl\text{-}2}$ cells treated with VP16 (*panel 3*) and CEM_{neo} cells treated with VP16 and ZVAD.FMK as described in Figure 2B, (*panel 4*) (**B** and **C**) Bar graphs showing the numerical summary of multi-parameter flow-cytometry experiments presented in Figure 4A. The bars are the same as described for Figure 4B and C

that Bcl-2 was unable to prevent cellular demise (data not shown). ZVAD.FMK-sensitive caspase inhibition was also able to greatly reduce cellular fragmentation (Figure 5A, panel 3; Figure 5C). Surprisingly however, ZVAD.FMK augmented VP16-induced loss of cell membrane integrity (Figure 5A, panel 4; Figure 5C). Together, these data indicate that Bcl-2 was able to prevent, or at least delay, all of the measured structural and morphological changes associated with apoptosis. In contrast, inhibition of ZVAD.FMK-sensitive caspases, while able to prevent chromatin condensation and cellular fragmentation, was unable to prevent the loss in cell membrane integrity and after VP16, ZVAD.FMK actually increased the number of cells which were permeable to propidium.

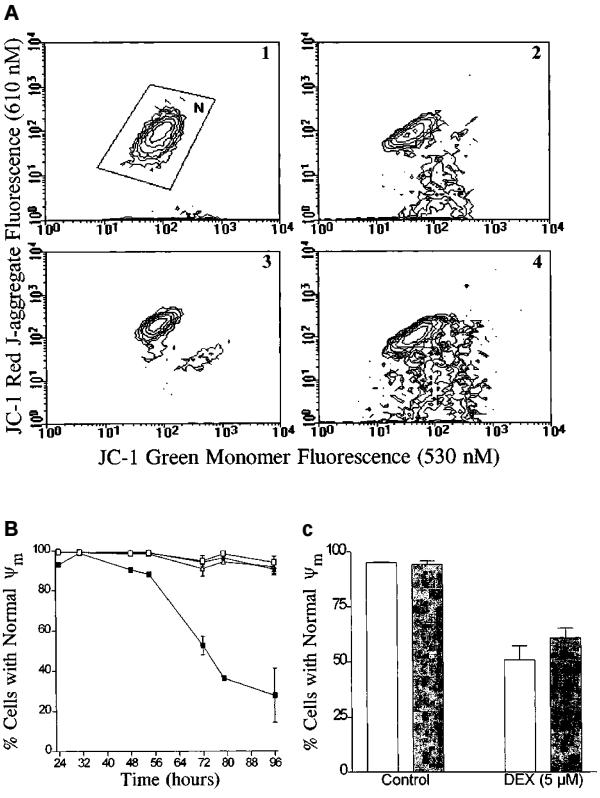

Figure 6 (**A**) The measurement of Ψ_M using multiparameter flow cytometry and the mitochondrial probe JC-1. Cells were incubated for 10 min with JC-1 (150 nM) at 37°C for 10 min. The cells were then washed in PBS and analyzed immediately. JC-1 fluorescence was acquired at 610 and 530 nm which corresponds to the J-aggregate and monomer fluorescence respectively. Loss of Ψ_M is detected as a decrease in the 610 fluorescence as shown in panels 2 and 4. CEM_{neo} cells were incubated for 72 h with 5 μM DEX (*panel 2 and 4*) or ethanol vehicle alone (*panel 1*). ZVAD.FMK was added as described in Figure 1B, (*panel 4*). $CEM_{Bcl\text{-}2}$ were also treated for 72 h with 5 μM DEX (*panel 3*). (**B**) Time course for the loss of Ψ_M in CEM cells treated with glucocorticoid for up to 96 h. CEM_{neo} (*squares*) or $CEM_{Bcl\text{-}2}$ cells (*triangles*) were treated with 5 μM DEX (*closed symbols*) or ethanol only (*open symbols*), acting as a vehicle control. The percentage of cells with normal Ψ_M was calculated by obtaining the number of events in the normal population gate shown in A. (**C**) Bar graph showing the effect of ZVAD.FMK on the percentage of cells with normal Ψ_M. Control and DEX treated cells were either incubated with DMSO (*white bars*) or ZVAD.FMK (*grey bars*) as described in Figure 1B. Data points for B and C represent the mean ± S.E.M. for three individual experiments

The effect of Bcl-2 and ZVAD.FMK on Ψ_M

Given this difference in the efficacy of ZVAD.FMK and Bcl-2 in preventing apoptotic cell membrane integrity loss and because cell membrane integrity is largely dependent on the energy charge of the cell (Hoffmann and Simonsen, 1989), we reasoned that Ψ_M may also be differentially protected by Bcl-2 and ZVAD.FMK. Figure 6 shows the effect of ZVAD.FMK and Bcl-2 on the DEX-induced Ψ_M loss. Dex alone induced a loss in Ψ_M (Figure 6A, panel 2). The number of cells displaying normal mitochondrial potentials decreased over the 96 h treatment period (Figure 6B). Bcl-2 was able to completely prevent this loss at all time points examined (Figure 6A, panel 3 and Figure 6B). In contrast, ZVAD.FMK was unable to prevent Ψ_M loss (Figure 6A, panel 4 and Figure 6C). This pattern was also observed after exposure to VP16. Here Bcl-2 suppressed Ψ_M loss even after 16 h of continuous exposure to the agent (Figure 7A, panel 3 and Figure 7B), while caspase inhibition by ZVAD.FMK was unable to prevent the

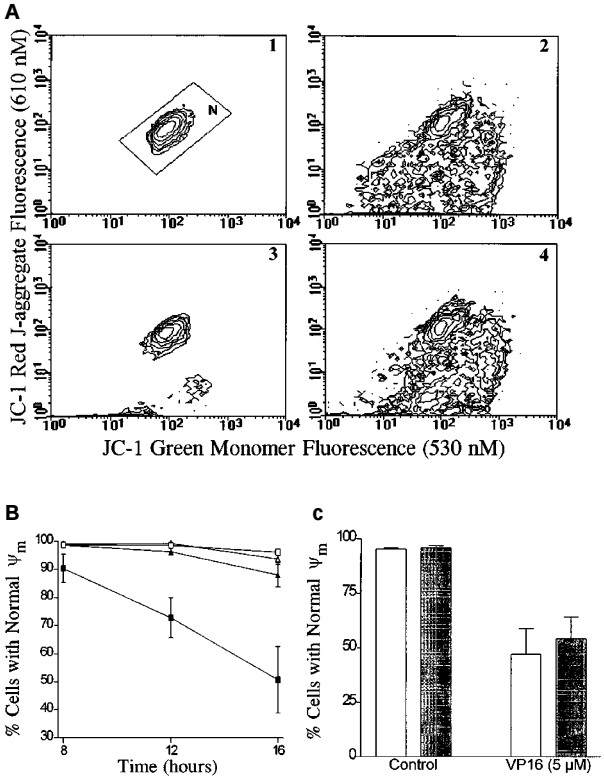

Figure 7 (**A**) The measurement of Ψ_M using multiparameter flow cytometry and the mitochondrial probe JC-1. Cells were incubated as described in Figure 6A. CEM_{neo} cells were incubated for 16 h with 5 μM VP16 (*panel 2 and 4*) or vehicle alone (*panel 1*). ZVAD.FMK was added as described in Figure 2B, (*panel 4*). $CEM_{Bcl\text{-}2}$ were also treated for 16 h with 5 μM VP16 (*panel 3*). (**B**) Time course for the loss of Ψ_M in CEM cells treated with etoposide for up to 16 h. CEM_{neo} (*squares*) or $CEM_{Bcl\text{-}2}$ cells (*triangles*) were treated with 5 μM VP16 (*closed symbols*) or DMSO : ethanol (1 : 20) only (*open symbols*), acting as a vehicle control. The percentage of cells with normal Ψ_M was calculated by obtaining the number of events in the normal population gate shown in A. (**C**) Bar graph showing the effect of ZVAD.FMK on the percentage of cells with normal Ψ_M. Control and VP16 treated cells were either incubated with DMSO (*white bars*) or ZVAD.FMK (*grey bars*) as described in Figure 2B. Data points for B and C represent the mean ± S.E.M. for three individual experiments

VP16-induced Ψ_M loss (Figure 7A, panel 4 and Figure 7C). The loss in Ψ_M and the onset of chromatin condensation follow similar kinetics after DEX or VP16 suggesting that Ψ_M loss must occur almost synchronously with the onset of chromatin condensation.

Discussion

Apoptosis, by definition is associated with a distinct cellular morphology (Arends and Wyllie, 1991). While dramatic changes such as chromatin condensation are an established part of apoptosis, it is not clear whether the other late structural changes, such cellular fragmentation, form an intrinsic part of the execution phase of the apoptotic programme or occur as a secondary consequence of cell death. The ability to block apoptosis at distinct levels allows such issues to be addressed. In this study, we examined the effect of Bcl-2 over-expression or ZVAD.FMK-sensitive caspase inhibition on several structural changes and on Ψ_M loss associated with apoptosis. Notably cell fragmentation and chromatin condensation can be blocked or attenuated by both Bcl-2 and ZVAD.FMK, however, cell death in terms of loss of plasma membrane integrity still occurs after etoposide (Figures 1, 2, 4 and 5). Moreover, etoposide treatment prevents clonogenic cell survival even in the presence of Bcl-2 over-expression (Lock and Stribinskiene, 1996; Brunet *et al*, 1997) demonstrating that CEM cell fragmentation is also inherent to the apoptotic programme and not a general consequence of cellular demise.

The striking difference between the action of ZVAD.FMK in the DEX and VP16 models pertains to its effects on membrane permeability. When treated with VP16 alone, the proportion of cells that were permeable to propidium remained extremely low (Figure 5C). However, when the apoptotic programme was blocked by ZVAD.FMK, the number of cells that were permeable to propidium greatly increased (Figure 5A, panel 4 and Figure 5C). In contrast, ZVAD.FMK did not change the number of cells permeable to propidium in DEX-induced apoptosis (Figure 4A, panel 4 and Figure 4C). A possible explanation for this discrepancy is that VP16 is intrinsically toxic causing DNA damage whereas DEX is not. Thus if caspase action is blocked by ZVAD.FMK, cells exposed to VP16 will still subsequently die, albeit by a non-apoptotic mechanism. These data are in agreement with a recent study which found that direct modulation of mitochondrial PT lead to apoptosis while inducing PT in the presence of ZVAD.FMK lead to a necrotic cell death (Hirsch *et al*, 1997). These data are also consistent with the idea that the plasma membrane is actively stabilized during apoptosis. Early studies suggested that the crosslinking of the protein $\epsilon(\mu$-glutamyl)lysine by the enzyme transglutaminase could mediate such an event (Fesus *et al*, 1991; Knight *et al*, 1991). Implicit in the data shown is that a caspase cleavage event may actually be required for membrane stabilisation during apoptosis.

Bcl-2 over-expression was able to prevent loss of cell membrane integrity in DEX-induced apoptosis. However, this is not surprising since clonogenic assays have demonstrated that Bcl-2 is able to inhibit the DEX-mediated cell death signal completely (Brunet *et al*, 1997). Moreover, Bcl-2 was able to delay the VP16-induced loss of membrane integrity which occurred beyond 16 h (data not shown). This demonstrates that Bcl-2 acts on other processes besides the inhibition the ZVAD.FMK-sensitive caspases. One possibility is that Bcl-2 maintains the energy charge of the cell which is known to be required for maintenance of plasma membrane integrity. Given the above results we investigated the effect of Bcl-2 and ZVAD.FMK inhibition of apoptosis on Ψ_M. We found that Bcl-2 but not ZVAD.FMK was able to prevent the loss in Ψ_M in both DEX and VP16-induced apoptosis. The correlation between the actions of ZVAD.FMK and Bcl-2 on Ψ_M and plasma membrane integrity at least suggests the possibility that the extra effects of Bcl-2 are in the modulation of intracellular energy levels which consequently affects the plasma membrane permeability of the cell. This idea seems even more plausible given the recent study which found that intracellular ATP levels influenced whether Jurkat cells treated with either CD95 or staurosporine died an apoptotic or necrotic death (Leist *et al*, 1997).

Another difference between the effects of Bcl-2 over-expression and inhibition of caspases was highlighted by our studies of cell shrinkage. Cell shrinkage is found in virtually all examples of apoptosis although its regulation and mechanism are poorly understood. However, in the DEX model, the situation is complicated since glucocorticoids induce a volume loss in two phases. Early volume loss begins well before the onset of chromatin condensation (Figure 1A). In a previous study of CEM-C7A cells we designated this as 'phase I'. This was in contrast to cell shrinkage which occurred concurrently with chromatin condensation which we designated as 'phase II' (Benson *et al*, 1996). Neither Bcl-2 nor ZVAD.FMK can prevent 'phase I' shrinkage even though Bcl-2 itself completely inhibits DEX-induced cell death as judged by clonogenicity (Brunet *et al*, 1997). Thus, it is likely that the first phase of volume loss in CEM cells treated with DEX is a glucocorticoid effect unrelated to killing. However, in both VP16 and DEX-induced apoptosis cell shrinkage which occurs concurrently with chromatin condensation was blocked by Bcl-2 over-expression. Surprisingly, ZVAD.FMK was unable to prevent dex-induced phase II shrinkage (Figure 1B) even though it did prevent cell shrinkage in VP16-induced apoptosis (Figure 2B). The reason for this difference is not clear although a possible explanation could be the presence of phase I cell shrinkage in DEX-induced apoptosis is confounding the detection of the inhibition of phase II shrinkage. Another possibility, is that the mechanisms which drive cell shrinkage in the DEX-model depend on activation caspases which are not inhibited by ZVAD.FMK. Finally, the mechanism which controls apoptotic cell shrinkage may be activated by several signals and the main signal used to activate it in VP16-induced apoptosis is caspase dependent, while in the DEX model the activation signal proceeds through a caspase independent pathway.

In this present study, we have examined several changes which occur in cells dying by apoptosis and evaluated the effect of inhibiting apoptosis by Bcl-2 over-expression or caspase inhibition on these changes. We found that cellular fragmentation, cell membrane integrity and cell volume are all modulated by the apoptotic programme. Furthermore, direct comparison of the inhibitory effects of Bcl-2 and ZVAD.FMK strongly suggest that the Bcl-2 prevention of cell death is more than simply the inhibition of ZVAD.FMK-sensitive caspases. Finally, these data demonstrate that while ZVAD.FMK can inhibit apoptosis as defined by morphology and chromatin condensation, it does not prevent cell death as defined by loss of plasma membrane integrity (allowing uptake of propidium). Similar conclusions have been drawn through the study of BAX and BAK-induced cell death (Xiang *et al*, 1996; McCarthy *et al*, 1997). In conclusion, the idea that all apoptotic-inducing death stimuli only induce apoptosis is too simplistic. Rather, some death stimuli, while inducing apoptosis will, if the programme is defeated, produce a more chaotic death which has features in common with necrosis. However, proteins such as Bcl-2 which heretofore have been thought of as only apoptotic modulators may also influence the development and kinetics of this second type of cellular demise.

Materials and Methods

Unless otherwise stated all culture media and supplements were purchased from Life Technologies (Paisley, Scotland, UK), fluorescent probes from Molecular Probes Inc. (Eugene, OR) and all other materials from Sigma Ltd (Poole, UK). CEM_{neo} and $CEM_{Bcl\text{-}2}$ cells, stably transfected with the retro-viral vectors pZipNeo and pZipBcl-2 respectively, were kindly provided by Dr Seamus Martin (La Jolla Institute for Allergy and Immunology, La Jolla CA, USA). Experiments using the cell lines were performed on cells of passage number 3–20. Cells were maintained in a 5% CO_2 humidified incubator at 37°C in RPMI 1640 medium supplemented with 50 μg penicillin, 50 μg streptomycin per 500 ml, 1% glutamine and 10% foetal bovine serum (FBS). Cells were routinely seeded at a density of 1×10^5 cells/ml and passaged every 3 or 4 days. During experiments, cells in log phase (1×10^5/ml-5×10^5/ml) were exposed to 5 μM dexamethasone (DEX) or 5 μM etoposide (VP16). Stock solutions of DEX (5 mM) and VP16 (5 mM) were prepared in ethanol and DMSO respectively. Stock solutions of the tripeptide ICE-like protease inhibitor ZVAD.FMK (Enzyme System Products Inc., Dublin, CA, USA) or DEVD.FMK (Calbiochem San Diego, CA, USA) were prepared in DMSO at a concentration of 50 mM. ZVAD.FMK was used at a final culture concentration of 50 μM and this concentration has been shown previously to completely inhibit poly(ADP-ribose) polymerase (PARP) cleavage in CEM-C7A cells (Brunet *et al*, 1997). Vehicle control cultures received ethanol or DMSO at a concentration of 0.1% v/v.

Fluorescence microscopy

The nuclear morphology of CEM-C7A cells was examined after staining with acridine orange (AO, 5 μg/ml) using a Olympus BH2 RFCA fluorescence microscope as previously described (Wood *et al*, 1994). Apoptotic cells were classified as those with condensed and fragmented chromatin.

Coulter counter volume measurement

Cell volume was measured as previously described (Benson *et al*, 1996) using a Coulter Counter (ZM; Coulter Electronics, Inc., Luton) with a 70 μm orifice connected to an IBM compatible 80386 16 MHz computer on which a channeliser programme was run (The Nucleus, Oxford Instruments, High Wycombe, UK). Cell debris could be resolved as a separate peak from the main cell population, thus the percentage of particles constituting cell debris could be calculated as described previously (Benson *et al*, 1996).

Flow cytometry

Multiparameter flow-cytometric analysis of cell size, plasma membrane integrity and chromatin condensation was performed using a FACS Vantage flow cytometer (Becton-Dickinson, San Jose, CA) as described previously (Dive *et al*, 1992; Benson *et al*, 1996).

Measurement of Ψ_M using JC-1

Cell cultures between $2-8\times10^5$ cells/ml were incubated for 10 min at 37°C with JC-1 at a final dye concentration of 10 μg/ml. The cells were then washed once and resuspended in PBS. Analysis was performed on a FACS Vantage flow cytometer (Becton-Dickinson, San Jose, CA) equipped with an Enterprise laser (Innova Technology, Coherent Inc., Palo Alto, CA) using a method recently described (Brunet *et al*, 1997).

Video microscopy

Cells were observed by videomicroscopy in a chamber maintained at 37 ± 0.1°C. Images were obtained every 20 s. The end of shrinkage was either the point where the cell obtained a stable volume or when the cells started to fragment, whichever came earlier.

PARP cleavage

For each sample a lysate was prepared by sonicating cells in a lysing buffer (Chen *et al*, 1997) and 20 μg of protein separated by SDS–PAGE (7.5% resolving gel, 4.5% stacking gel) and transferred to a polyvinylidene difluoride (PVDF) membrane. The blot was blocked with 5% dried milk in PBS and then incubated for 2 h at 23°C with the primary antibody, murine anti-PARP, (kindly donated by Drs S Aoufouchi and Milstein, MRC Centre, Cambridge UK). The immunoreactive proteins were visualised using rabbit horse radish peroxidase conjugated anti-mouse-IgG (1:1000) and enhanced chemiluminescence (ECL).

Statistical analysis

Where applicable the data are presented as the mean$\pm$S.E.M. unless otherwise indicated. Comparison of means was performed by Student's unpaired *t*-test. A probability of 0.05 or less was considered significant.

Acknowledgements

We would like to thank Dr Terry Allen for his help with the videomicroscopy experiments, Bindy Heere for her assistance with flow cytometry, and Professor John Hickman and Dr Ged Brady for their helpful suggestions. CD is a Lister Research Fellow. This project was supported by a grant from the Wellcome Trust.

References

Arends MJ and Wyllie AH. (1991) Apoptosis: Mechanisms and roles in pathology. Int. Rev. Exp. Path. 32: 223 – 254

Benson RSP, Heer S, Dive C and Watson AJM. (1996) Characterisation of cell volume loss in CEM-C7A cells during dexamethasone-induced apoptosis. Am. J. Physiol. 270: C1190 – C1203

Boise LH and Thompson CB. (1997) Bcl-x_L can inhibit apoptosis in cells that have undergone FAS-induced protease activation. Proc. Natl. Acad. Sci. 94: 3759 – 3764

Brunet CL, Gunby RH, Benson RSP, Hickman JA, Watson AJM and Brady G. (1997) Commitment to clonogenic BCL-2-regulated cell death in a human lymphoid cell line is unaffected by caspase inactivation. Cell Death Differ. 5: 107 – 115

Chen QC, Benson RSP, Whetton AD, Brant SR, Donowitz M, Montrose MH, Dive C and Watson AJM. (1997) Role of acid/base homeostasis in the suppression of apoptosis in haemopoietic cells by v-Abl protein tyrosine kinase. J. Cell Sci. 110: 379 – 387

Cohen GM. (1997) Caspases: the executioners of apoptosis. Biochemical Journal 326: 1 – 16

Decaudin D, Geley S, Hirsch T, Castedo M, Marchetti P, Macho A, Reinhard K and Kroemer G. (1997) Bcl-2 and Bcl-X_L antagonize the mitochondrial dysfunction preceding nuclear apoptosis induced by chemotherapeutic agents. Cancer Res. 57: 62 – 67

Dive C, Gregory CD, Phipps DJ, Evans DL, Milner AE and Wyllie AH. (1992) Analysis and discrimination of necrosis and apoptosis (programmed cell death) by multiparameter flow cytometry. Biochim. Biophys. Acta. 1133: 275 – 285

Fesus L, Thomázy V and Falus L. (1991) Induction and activation of tissue transliterations during programmed cell death. FEBS Lett. 224: 104 – 108

Golstein P. (1997) Controlling cell death. Science 275: 1081 – 1082

Hirsch T, Marchetti P, Susin SA, Dallaporta B, Zamzami N, Marzo I, Geuskens M and Kroemer G. (1997) The apoptosis-necrosis paradox, Apoptogenic proteases activated after mitochondrial permeability transition determine the mode of cell death. Oncogene 15: 1573 – 1581

Hoffmann EK and Simonsen LO. (1989) Membrane mechanisms in volume and pH regulation in vertebrate cells. Physiol. Rev. 69: 315 – 382

Kluck RM, Bossy-Wetzel E, Green, DR and Newmeyer D. (1997) The release of cytochrome c from mitochondria: a primary site for bcl-2 regulation of apoptosis. Science 275: 1132 – 1136

Knight CRL, Ress RC and Griffin M. (1991) Apoptosis: a potential role for cytosolic transglutaminase and its importance in tumour progression. Biochim. Biophys. Acta. 1096: 312 – 318

Kroemer G. (1997) The proto-oncogene Bcl-2 and it role in regulating apoptosis. Nature Med. 3: 614 – 619

Leist M, Single B, Castoldi AF, Kühnle S and Nicotera P. (1997) Intracellular adenosine triphosphate (ATP) concentration: a switch in the decision between apoptosis and necrosis. J. Exp. Med. 185: 1481 – 1486

Lock RB and Stribinskiene L. (1996) Dual modes of death induced by etoposide in human epithelial tumor cells allow bcl-2 to inhibit apoptosis without affecting clonogenic survival. Cancer. Res. 56: 4006 – 4012

McCarthy NJ, Whyte MK, Gilbert CS and Evan GI. (1997) Inhibition of Ced-3/ICE-related proteases does not prevent cell death induced by oncogenes, DNA damage, or the Bcl-2 homologue Bak. J. Cell. Biol. 136: 215 – 227

Meisenholder GW, Martin SJ, Green DR, Nordberg J, Babior BM and Gottlieb RA. (1996) Events in apoptosis: acidification is downstream of protease activation and bcl-2 protection. J. Biol. Chem. 271: 16260 – 16262

Oltvai ZN and Korsmeyer SJ. (1994) Checkpoints of duelling dimers foil death wishes. Cell 79: 189 – 192

Slee EA, Zhu H, Chow SC, MacFarlane M, Nicholson, DW and Cohen GM. (1996) Benzyloxycarbonyl-Val-Ala-Asp (Ome) fluoromethylketone (Z-VAD.FMK) inhibits apoptosis by blocking the processing of CPP32. Biochemical Journal 315: 21 – 24

Wood AC, Waters CM, Garner A and Hickman JA. (1994) Changes in c-*myc* expression and the kinetics of dexamethasone-induced programmed cell death (apoptosis) in human lymphoid leukaemia cells. Brit. J. Can. 69: 663 – 669

Xiang J, Chao DT and Korsmeyer SJ. (1996) BAX-induced cell death may not require interleukin 1 beta-converting enzyme-like proteases. Proc. Natl. Acad. Sci. USA 93: 14559 – 14563

Yang J, Liu X, Bhalla K, Kim CN, Ibrado AM, Cai J, Peng TI, Jones DP and Wang X. (1997) Prevention of apoptosis by Bcl-2 release of cytochrome c from mitochondria blocked. Science 275: 1129 – 1132

Zamzami N, Marchetti P, Castedo M, Zanin C, Vayssiere JL, Petit PX and Kroemer G. (1995) Reduction in mitochondrial potential constitutes an early irreversible step of programmed lymphocyte death in vivo. J. Exp. Med. 181: 1661 – 1672

Zamzami N, Susin SA, Marchetti P, Hirsch T, Gómez-Monterrey I, Castedo M and Kroemer G. (1996) Mitochondrial control of nuclear apoptosis. J. Exp. Med. 183: 1533 – 1544.